Liquid Crystals
Publication details, including instructions for authors and subscription information:
http://www.informaworld.com/smpp/title~content=t713926090

New switchable smectic phases in banana-shaped compounds

J. P. Bedel; J. C. Rouillon; J. P. Marcerou; M. Laguerre; H. T. Nguyen; M. F. Achard

Online publication date: 06 August 2010

To cite this Article Bedel, J. P. , Rouillon, J. C. , Marcerou, J. P. , Laguerre, M. , Nguyen, H. T. and Achard, M. F.(2001) 'New switchable smectic phases in banana-shaped compounds', Liquid Crystals, 28: 9, 1285 — 1292
To link to this Article: DOI: 10.1080/02678290110039949
URL: http://dx.doi.org/10.1080/02678290110039949

LIQUID CRYSTALS, 2001, VOL. 28, NO. 9, 1285–1292

New switchable smectic phases in banana-shaped compounds

J. P. BEDEL, J. C. ROUILLON, J. P. MARCEROU, M. LAGUERRE†,
H. T. NGUYEN and M. F. ACHARD*

Centre de Recherche Paul Pascal, Université Bordeaux I, Av. A. Schweitzer,
33600 Pessac, France
†Institut Européen de Chimie et Biologie,
Ecole Polytechnique-Université Bordeaux I-Université Bordeaux II,
Avenue Pey-Berland, 33402 Talence, France

(*Received 8 November 2000; accepted 19 December 2000*)

A new series of achiral compounds with banana-shaped molecules ('E_n') has been synthesized and studied by the classical techniques (optical microscopy, differential scanning calorimetry, X-ray diffraction, miscibility studies and electro-optic investigations). The short homologues (E_7–E_{10}) give switchable smectic mesophases. Nevertheless their textures clearly differ from those of the B2 mesophase. In addition, the E_{10} compound displays a smectic polymorphism involving a new bilayered structure.

1. Introduction

Banana-shaped liquid crystal molecules represent a new subfield of liquid crystals since the mesophases encountered are specific for molecules of this shape and have no counterpart in the field of calamitic mesogens. According to the recommendations of the Workshop on Banana-Shaped Liquid Crystals: Chirality by Achiral Molecules, held in Berlin in 1997, these phases are simply designated by 'B*n*' (where *n* corresponds to the sequence of their discovery). These materials form different smectic phases, but also two-dimensional phases. In this sense, this nomenclature remains very preliminary, since it does not take into account the structure and symmetry of the mesophases.

As a result of their bent-shape, several arrangements of the molecules can be imagined: Brand *et al.* have described different possibilities for the packing of bent molecules within a smectic layer [1]. Moreover, intercalated or bilayer smectic structures can constitute variants to this basic description of a simple layer. As a consequence, several smectic phases can exist in these banana-shaped compounds. Up to now, different smectic B*n* phases have been detected which have no in-plane order according to X-ray measurements and several of them can be electro-optically switched.

*Author for correspondence;
e-mail: achard@crpp.u-bordeaux.fr

The most frequently investigated smectic phase is the B2 phase which gives an antiferroelectric switching [2, 3]. The B5 phase has an additional short range order within the layers, but keeps the same electro-optic response as the B2 phase [4]. An intercalated smectic phase (B6), with a layer spacing smaller than half the length of the molecule, has been observed in one compound, but no evidence for the electro-optic response has been given [2]. In most cases, each compound exhibits only one smectic phase. However, we recently reported a thiobenzoate series [5] with a complex smectic polymorphism showing four successive switchable phases. Their textures clearly differ from those of a B2 phase. In a compound with a lateral fluoro substituent on the phenyl rings adjacent to the terminal aliphatic tails [6] or with sulfur containing tails [7], a smectic phase with spiral defects similar to the B7 two-dimensional mesophase [8] and with antiferroelectric switching has been reported.

All these examples underline the difficulty in the assignment of the mesophases of new banana compounds by reference to the nomenclature system adopted at the Workshop on Banana-Shaped Liquid Crystals. Indeed, at this moment it is difficult to establish a direct relationship between observed textures, structural peculiarities and phase assignment

We present here a new series of banana compounds which exhibits smectic phases for the short homologues.

Liquid Crystals ISSN 0267-8292 print/ISSN 1366-5855 online © 2001 Taylor & Francis Ltd
http://www.tandf.co.uk/journals
DOI: 10.1080/02678290110039949

2. Materials

These new symmetric banana-shaped molecules (series 'E_n') correspond to the general formula:

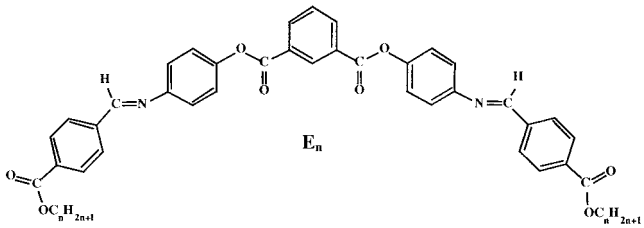

The materials are labelled E_n, where n is the number of carbon atoms in the terminal ester chain ($n = 7$–10). In these molecules, ester groups are linked to the 1,3-positions of the central phenyl ring and the azomethine groups are placed between the outside phenyl rings. They differ from the P-*n*OPIMB references series [9] in the nature of the terminal chains and in the directional sense of the connecting groups between the aromatic rings which are reversed. As previously mentioned, the alternating distribution of the charges on the five phenyl rings is respected according to our molecular architectural model [5, 10], and even emphasized by the acceptor nature of the terminal ester linkage.

3. Synthesis

The members of the bis4-(4-*n*-alkyloxycarbonylbenzylideneamino)phenyl isophthalate series (series E_n) were synthesized according to the scheme in figure 1.

The appropriate *n*-alkanol (0.01 mol) in dichloromethane (CH_2Cl_2) was interacted with 4-carboxybenzaldehyde (0.01 mol) in the presence of dicyclohexylcarbodiimide (DCC) (0.011 mol) and 4-dimethylaminopyridine (DMAP) as catalyst. The solution was stirred at room temperature for about 24 h. This esterification led to the *n*-alkyl 4-formylbenzoate (1E), which was chromatographed on silica gel with 9 : 1 heptane-ethyl acetate as eluent. The product 1E (5 mmol) and 4-aminophenol (5 mmol) were dissolved in boiling absolute ethanol in the presence of a few drops of acetic acid. The mixture was heated at reflux, with stirring, for 3 h. The 4-(4-*n*-alkyloxycarbonylbenzylideneamino)phenol (2E) obtained from this condensation was recrystallized three times from heptane. To obtain the members of the E_n series, the required compound 2E (2 mmol) was dissolved in CH_2Cl_2 with DCC (2.2 mmol) and DMAP as catalyst, and interacted with isophthalic acid (1 mmol). The solution was stirred at room temperature for about 24 h. The products were recrystallized three times from an ethanol/toluene mixture and twice from a toluene/heptane mixture; yields 30–50%.

The following analytical data for E_{10} are given as representative of the homologous series: ^{1}H NMR ($CDCl_3$) δ (ppm): 0.9 (m, 6H, 2 CH3), 1.3 (m, 28H, 14 CH_2), 1.8 (m, 4H, 2 COO−CH_2−$\underline{CH_2}$), 4.35 (t, 4H, 2 COO−$\underline{CH_2}$), 7.3 (m, 8H, Ar−H), 7.7 (t, 1H, Ar−H), 7.95 (d, 4H, Ar−H), 8.15 (d, 4H, Ar−H), 8.5 (m, 4H, 2 CH=N and 2Ar−H), 9.05 (s, 1H, Ar−H).

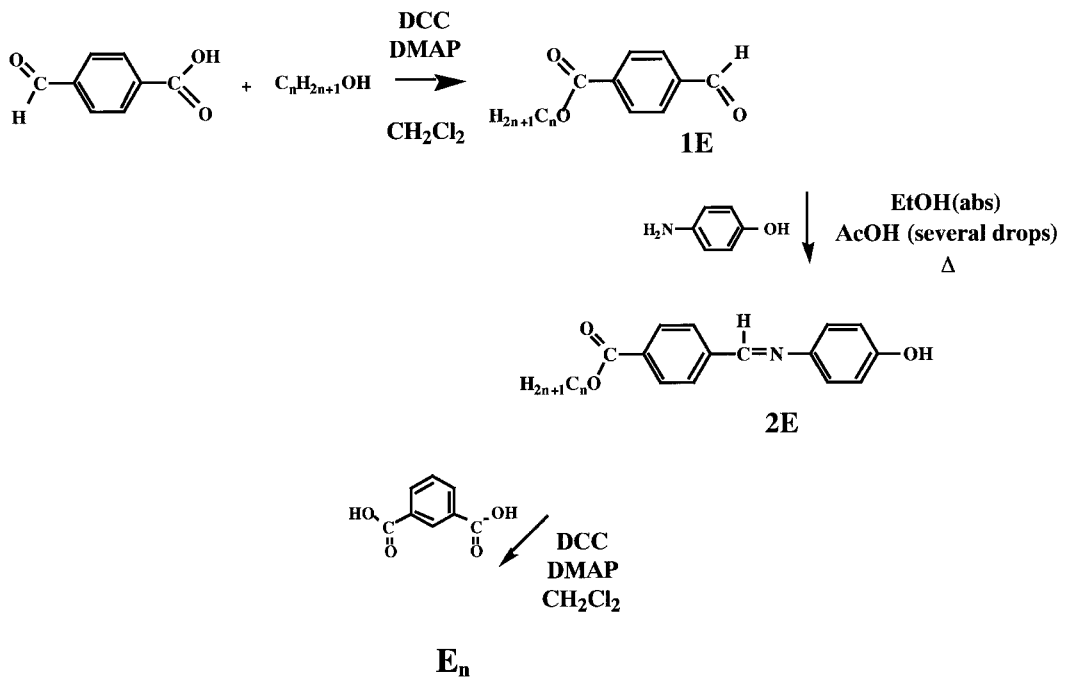

Figure 1. Synthesis scheme.

4. Characterization

The thermal behaviour of the materials was investigated using a Perkin-Elmer DSC7 differential calorimeter. The optical textures of the mesophases were observed using a polarizing microscope (Leitz Diavert) equipped with a hot stage (FP-82HT) and an automatic controller (Mettler FP-90). Samples were observed on regular slide glass without any surface treatment.

X-ray diffraction experiments were carried out using an 18 kW rotating anode X-ray source (Rigaku-200) and a Ge(1 1 1) crystal as monochromator. The scattered radiation was collected on a two-dimensional detector (imaging plate system from Mar Research, Hamburg). The samples were placed in an oven, providing a temperature control of 0.1 K. Oriented samples of the smectic phases were obtained by slow cooling of a drop of the isotropic liquid.

Electro-optical properties were studied using commercial cells (from EHC, Japan) with rubbed polyimide layers (but the surface treatment is not effective for obtaining uniformly oriented cells). Switching current was observed by applying a voltage-wave using a function synthesizer (HP 331 20A) and a high power amplifier (Krohn-Hite).

5. Results and discussion

The microscopic textural observations and the X-ray analysis show that several mesophases exist dependent on the chain lengths. The homologues with the shortest chains (E_7–E_9) exhibit one smectic phase Sm_1. Two smectic phases, Sm_1 and Sm_2, are seen for the E_{10} compound. The transition temperatures and associated enthalpies for this series are reported in the table.

Table. Transition temperatures (°C) and enthalpies (italics, kJ mol^{-1}) as a function of the carbon atom number in the terminal chains (from DSC runs, increasing temperature, rate 5°C min^{-1}).

n	Cr		Sm_0		Sm_1		I
7	•	183.9 *43.8*	•	190.6 *19.7*	—		•
8	•	178.6 *37.0*	•	187.8 *18.9*	—		•
9	•	174.0 *36.8*	•	184 *20.3*	—		•
10	•	173.5 *40.8*	•	180 *0.2*	•	183.5 *20.4*	•

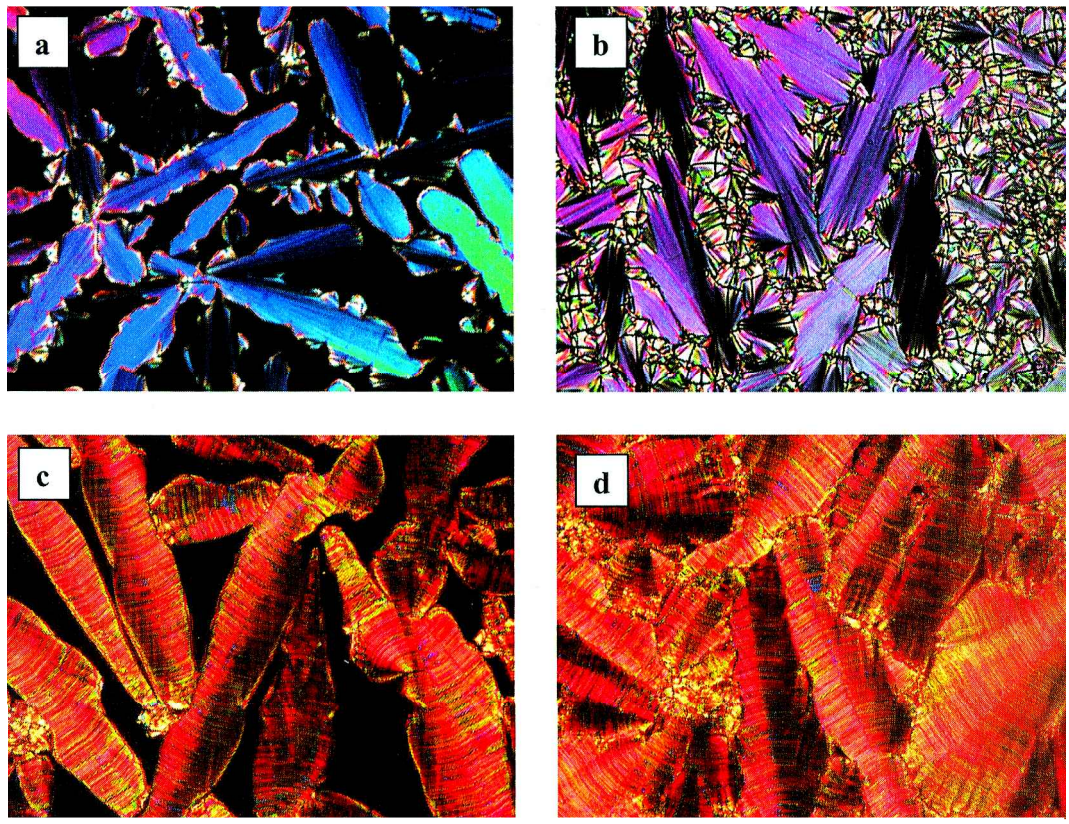

Figure 2. Textures of the mesophase Sm_0: (*a*) E_7 at 187.5°C, (*b*) E_7 at 177°C, (*c*) E_9 at 180°C, (*d*) E_9 at 176°C.

5.1 *Microscopic observations*

On cooling the isotropic state, the mesophase Sm_0 grows as dendrites or coloured rods. Stripes generally appear perpendicular to the lengthening direction. Typical textures of this phase are shown in the figure 2.

The photomicrographs of the Sm_1 phase of the E_{10} homologue obtained by slow cooling from the isotropic state show microscopic 'spiral domains', figure 3 (*a*), which suggest the presence of helical superstructure as observed in other banana-shaped compounds [6–8, 11, 12]. On further cooling, a fan-shaped texture is observed, figure 3 (*b*), and the Sm_1–Sm_0 transition is clearly put in evidence by the appearance of transverse striations on the fan shaped regions, figure 3 (*c*). The E_9–E_{10} binary phase diagram confirms that the low temperature mesophase of the compound E_{10} is miscible with the Sm_0 phase of the E_9 homologue.

5.2. *X-ray analysis*

The X-ray patterns of Sm_0 show equally spaced Bragg reflections giving evidence of a layer structure. In addition, a broad diffuse scattering in the wide angle region indicates a fluid smectic with no long range positional order within the layers. Oriented monodomains were obtained by slow cooling of a free droplet from the isotropic state; such a pattern is shown in figure 4 for E_8. The Bragg reflections corresponding to the wave vector q and their higher orders ($2q$, $3q$) are located on the meridian of the pattern. The diffuse maxima at wide angles are situated out of the equator, indicating a tilt of the molecules. The tilt angle was estimated to be 25°, which is smaller than the tilt angle of the molecules in the B2 phase (35° to 40°) in different series of banana-shaped compounds [3, 6, 13]. Such patterns are consistent with a smectic phase with tilted molecules without in-plane order within the layers. The layer thickness is not temperature dependent in the Sm_0 phase: 42.2 Å for E_7 ($q = 0.149$ Å^{-1}), 43.9 Å for E_8 ($q = 0.143$ Å^{-1}), 44.9 Å for E_9 ($q = 0.140$ Å^{-1}) and 46.5 Å for E_{10} ($q = 0.135$ Å^{-1}). In addition, the evolution of the layer spacing d from E_7 to E_{10} may be fitted by $d = (32.4 + 1.40n)$ Å, where n is the carbon number in each terminal chain. The increment in d is lower than that expected per methylene group, suggesting that the chains are tilted with reference to the smectic layers.

The oriented pattern of the high temperature Sm_1 phase of E_{10} shows an additional reflection of low intensity at $q/2 = 0.068$ Å^{-1}, while the intense reflection

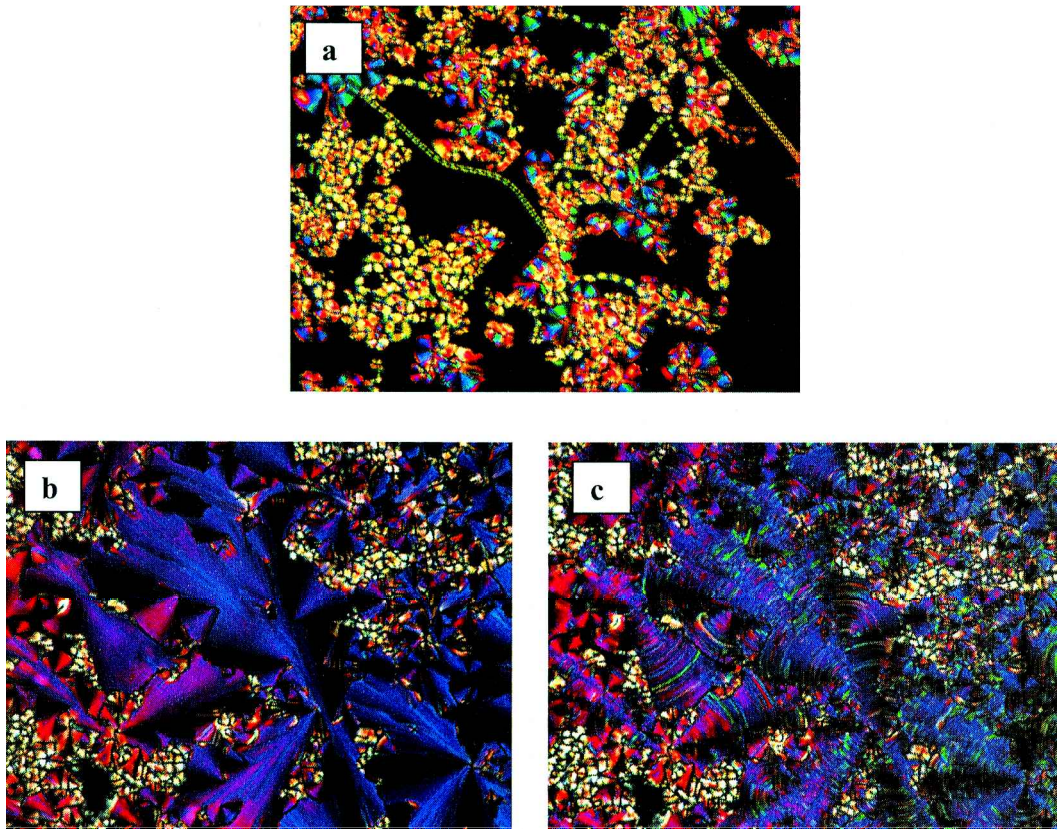

Figure 3. Textures of the mesophases of E_{10}: (*a*) Sm_1 phase on slow cooling from the isotropic state (181°C), (*b*) Sm_1 phase at 175°C, (*c*) Sm_0 phase at 166°C.

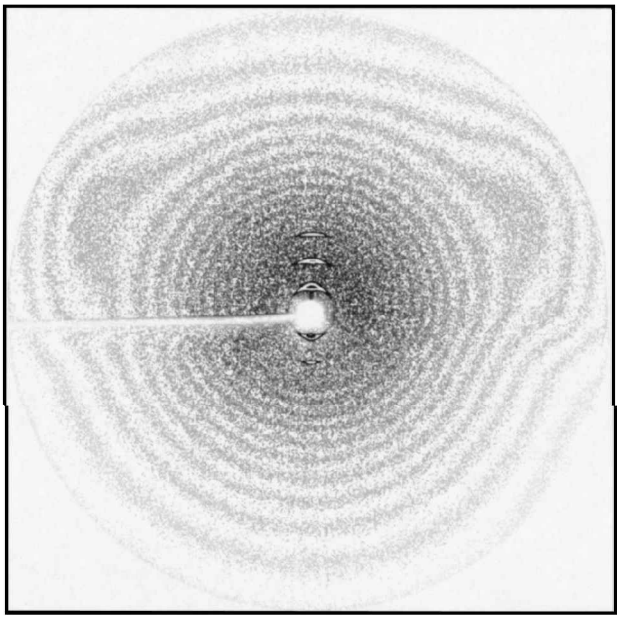

Figure 4. X-ray pattern of a monodomain of the Sm_0 phase of E_8 (178°C). The use of iso intensity curves allows a better sighting of the diffuse maxima at wide angle. The free droplet geometry prevents access to the lower part of the pattern at wide angle.

at $q = 0.136$ Å^{-1} remains with its harmonic at $2q$ (figure 5). This Sm_1 mesophase thus corresponds to a bilayer smectic phase with a layer spacing of 92 Å. The Sm_1–Sm_0 phase transition induced by decreasing temperature is characterized by the disappearance of the $q/2$ reflection and so corresponds to a 'bilayer–monolayer' structural change. To our knowledge, it is the first example of a bilayer smectic phase in banana compounds.

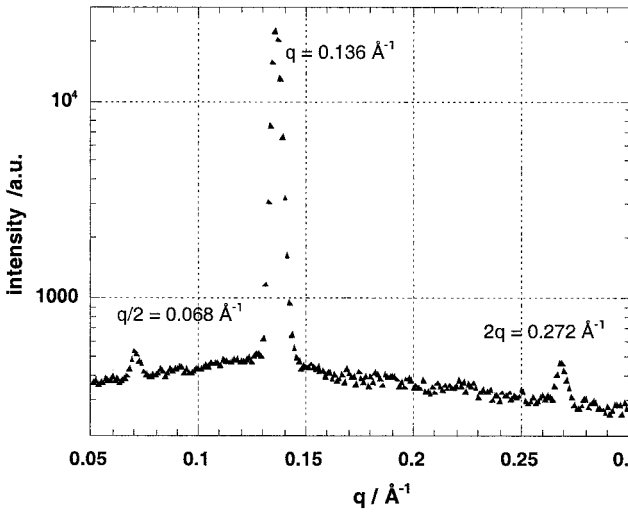

Figure 5. Intensity profile corresponding to the oriented X-ray pattern of the Sm_1 phase of E_{10} (182°C).

5.3. *Electro-optic studies*

The mesophase Sm_0 shows electro-optic switching. By applying a triangular voltage, a single peak per half-period was observed in the switching current response, above a threshold of 2.5 V μm^{-1}; see figure 6 (*a*). Nevertheless, one can see that the switching starts before the applied voltage reaches 0 V, which means the switching takes place between $-V$ and 0 V and between 0 V and $+V$. By applying a modified triangular voltage with plateaux at $-V$, 0 V and $+V$, previously described in [11], two peaks per half-period were observed, which is the signature of an 'antiferroelectric' type switching; see figure 6 (*b*). In this phase, the polarization is annihilated just before the applied voltage reaches 0 V, when the electric field goes from $-V$ to 0 V (or respectively from $+V$ to 0 V), and the polarization is created just after 0 V, when the electric field goes from 0 V to $+V$ (or respectively from 0 V to $-V$). The response times are not equivalent depending on the sense of the applied electric field, and with the classical triangular voltage wave method, the two peaks in the switching current response are not separated. The polarization value was estimated to be about 600 nC cm^{-2}.

Above the switching threshold a colour change was clearly observed in the sample texture. For E_7, the sample is more or less yellow below the threshold and becomes purple above it. It is noticeable that the two states under positive and negative electric fields cannot be distinguished by polarizing optical microscopy. Thus, there is no difference in the average optical axis in the sample between these two states.

In the case of E_{10}, the high temperature smectic phase Sm_1 also shows antiferroelectric switching above a threshold field of 3 V μm^{-1}. The polarization value (300 nC cm^{-2}) of the bilayer Sm_1 figure 7 (*a*), is lower than in the low temperature monolayer Sm_0 phase (550 nC cm^{-2}), figure 7 (*b*).

The optical textures of the Sm_0 and Sm_1 mesophases under an applied electric field also differ clearly from those of the B2 phase for which a striped texture is observed [3, 14]. In addition, in the case of a B2 phase, a ferroelectric hump is observed in the switching current response below the antiferrolectric response threshold [3, 14], which is not the case here for the Sm_0 and Sm_1 phases.

5.4. *Miscibility studies*

We can conclude that the mesophase Sm_0 is a 'monolayer' smectic phase with an optical texture very different from the B2 phase, but with an 'antiferroelectric'-type electro-optic response. Therefore it was interesting to compare these two phases. For this purpose, the binary phase diagram between the homologue E_9 and the reference compound P-8OPIMB showing a B2 phase

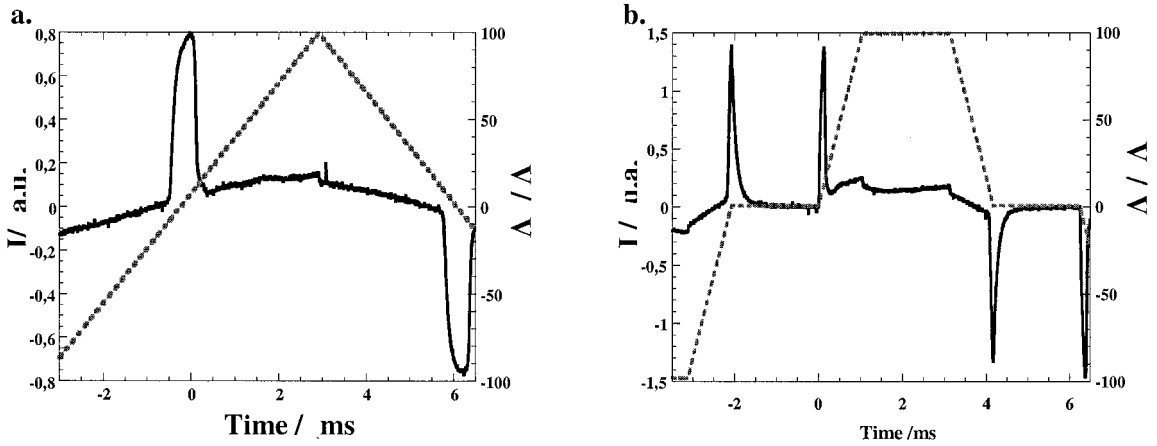

Figure 6. Switching current response in the Sm_0 mesophase of E_7 at 177°C: (*a*) by applying a triangular voltage (± 28.6 V μm^{-1}, 80 Hz); (*b*) by applying a modified triangular voltage, with plateaux (± 28.6 V μm^{-1}, 80 Hz).

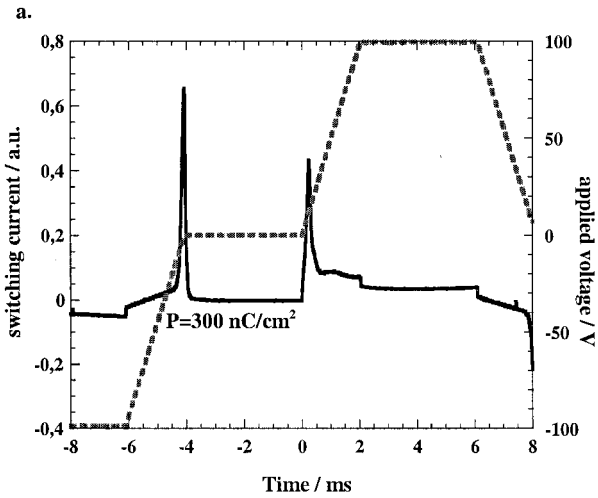

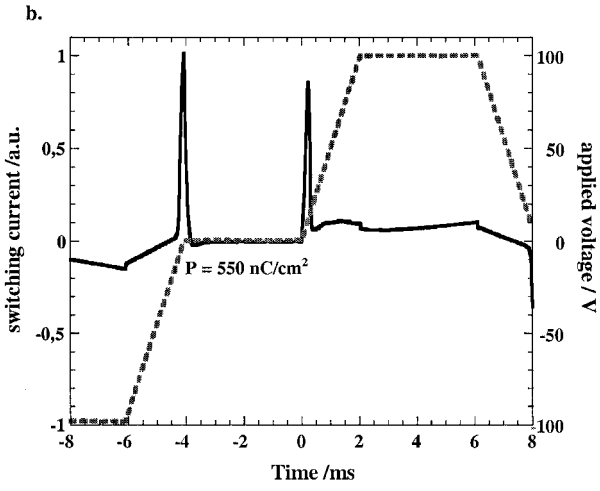

Figure 7. Switching current response in the two mesophases of compound E_{10} obtained by applying a modified triangular voltage with plateaux (± 28 V μm^{-1}, 40 Hz): (*a*) Sm_1 phase, (*b*) Sm_0 phase.

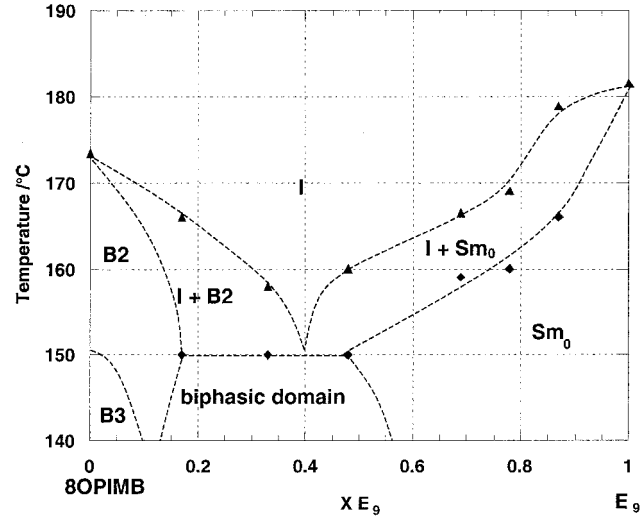

Figure 8. Binary phase diagram between P-8OPIMB which has a B2 mesophase (left) and $\mathbf{E}_9$ (right). A large biphasic domain separates the B2 phase and the Sm_0 phase of E_9. This smectic–smectic phase separation is characterized by the coexistence of two wave vectors: for $xE_9 = 0.20$, $q = 0.131$ and $0.158\ Å^{-1}$; for $xE_9 = 0.33$, $q = 0.133$ and $0.146\ Å^{-1}$; for $xE_9 = 0.48$, $q = 0.135$ and $0.140\ Å^{-1}$. By comparison, in the monophasic B2 domain $q = 0.162\ Å^{-1}$, and in the Sm_0 domain $q = 0.140\ Å^{-1}$ for pure E_9 and $q = 0.137\ Å^{-1}$ for $xE_9 = 0.78$.

has been studied. This diagram results from complementary techniques: microscopic observations, DSC measurements and X-ray analysis of mixtures at given concentrations.

As shown in figure 8, this diagram presents three main characteristics: (1) very large isotropic liquid/mesophase biphasic domains easily seen under the microscope; (2) a non-linear evolution of the clarification temperature with a deep minimum indicating the low compatibility

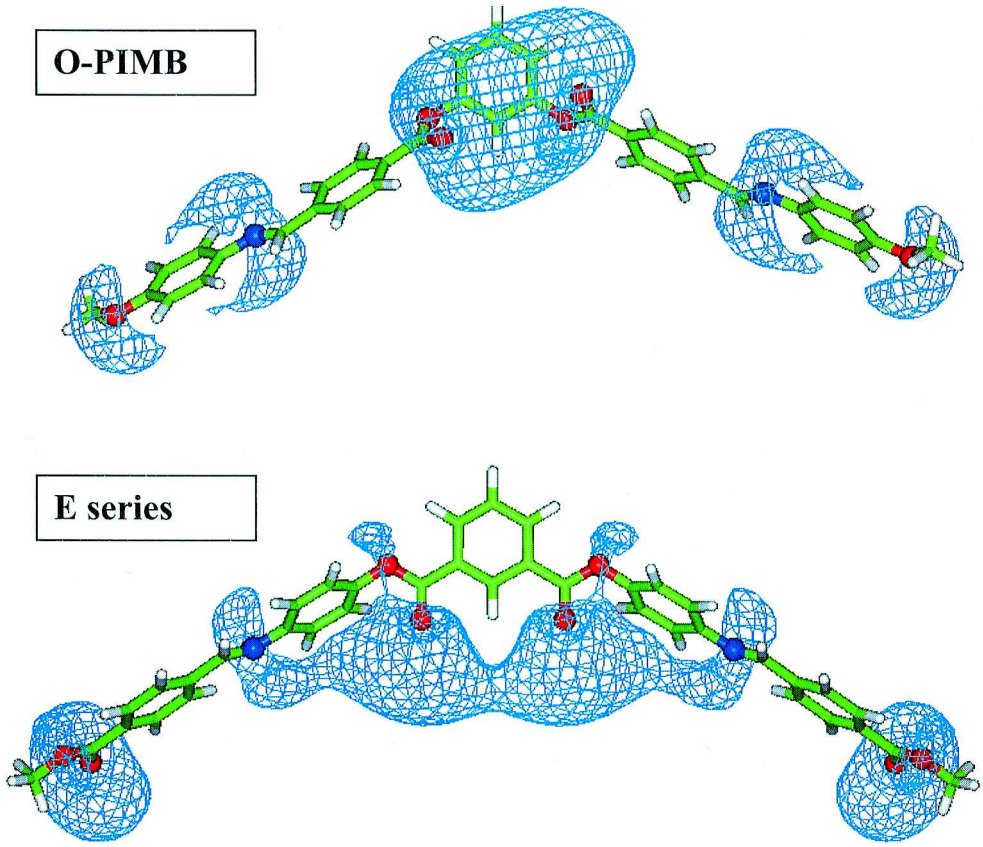

Figure 9. Configuration of O-PIMB and E compounds resulting from MD and electrostatic potential calculations showing the repartition of the negative potential (blue contours at $-40\,kJ\,mol^{-1}$) along the molecules.

of the two compounds; (3) the appearance in the mesomorphic range of a wide domain of phase separation confirming the incompatibility of the components. The B2 and Sm_0 mesophases are thus separated by a biphasic domain, clearly evidenced by the coexistence of two smectic parameters extending over a large concentration range (for wave vectors see figure 8). Therefore, the mesophases of these two compounds are incompatible. As illustrated by the electrostatic potential maps of figure 9, the rotation about the linking groups strongly modifies the repartition of charge density from PIMB to the E_n series and this modification may be sufficient to generate the incompatibility of the smectic structures. In this situation, one cannot exclude the possibility that both phases belong to the same type. Nevertheless, we have recently demonstrated the complete miscibility of the B2 mesophase the PIMB series with the B2 phase of the 'C_n' series corresponding to a reversed sequence of charge density by comparison with PIMB molecules. Despite this change, the behaviour of the binary solutions appears almost ideal and the clearing equilibrium line shows only a very slight curvature; the structural parameters evolve continuously along it [3].

In the present case, these observations and the clear textural difference between the B2 and the Sm_0 phases, lead us to think that these two phases are different, but we are without definitive proof. Nevertheless, the Sm_1 phase of the E_{10} homologue is indubitably a new switchable smectic phase with a bilayer structure, and a bilayer–monolayer phase transition is observed for the first time for this compound. For this reason and according to the recommendations of the Workshop on Banana-Shaped Liquid Crystals (Berlin 1997), we suggest naming the Sm_1 phase 'B8'.

References

[1] Brand, H. R., Cladis, P. E., and Pleiner, H., 1998, *Eur. Phys. J.*, **B6,** 347.

[2] See for example: Pelzl, P. G., Diele, S., and Weissflog, W., 1998, *Adv. Mater.*, **11,** 707 and the references therein.

[3] Bedel, J. P., Rouillon, J. C., Marcerou, J. P., Laguerre, M., Achard, M. F., and Nguyen, H. T., 2000, *Liq. Cryst.*, **27,** 103.

[4] Diele, S., Grande, S., Kruth, H., Lischka, C., Pelzl, G., Weissflog, W., and Wirth, I., 1998, *Ferroelectrics*, **212,** 169.
[5] Nguyen, H. T., Rouillon, J. C., Marcerou, J. P., Bedel, J. P., Barois, P., and Sarmento, S., 1999, *Mol. Cryst. liq. Cryst*., **328,** 177.
[6] Heppke, G., Parghi, D. D., and Sawade, H., 2000, *Ferroelectrics*, **243,** 269.
[7] Heppke, G., Parghi, D. D., and Sawade, H., 2000, *Liq. Cryst*., **27,** 313.
[8] Pelzl, G., Diele, S., Jakli, A., Lischka, C., Wirth, I., and Weissflog, W., 1999, *Liq. Cryst*.. **26,** 135.
[9] Niori, T., Sekine, T., Watanabe, J., Furukawa, T., and Takezoe, H., 1996, *J. Mater. Chem*., **6,** 1231.
[10] Nguyen, H. T., Rouillon, J. C., Marcerou, J. P., and Barois, P., 1999, in Abstracts of the 17th International Liquid Crystal Conference, Strasbourg, D2-O3.
[11] Bedel, J. P., Rouillon, J. C., Marcerou, J. P., Laguerre, M., Nguyen, H. T., and Achard, M. F., 2000, *Liq. Cryst*., **27,** 1411.
[12] Wang Lee, C.-K., and Chien, L.-L., 1999, *Liq. Cryst*., **26,** 609.
[13] Pelzl, G., Diele, S., Grande, S., Jakli, A., Lischka, Ch, Kresse, H., Schmalfuss, H., Wirth, I., and Weissflog, W., 1999, *Liq. Cryst*., **26,** 401.
[14] Link, D. R., Natale, G., Shao, R., Maclennan, J. E., Clark, N. A., Korblova, E., and Walba, D. M., 1997, *Science*, **278,** 1924.